Adaptive attitude control of uncertain spacecraft with attitude and angular velocity constraints

Zeyu Kang[1], Shufan Wu[1,3], Xiaoliang Wang[1], Chao Zhong[2], and Qiang Shen[1]

[1] Shanghai Jiao Tong University, Shanghai, 200240, P. R. China
{kangzeyu, shufan.wu, xlwang12321, qiangshen}@sjtu.edu.cn,
[2] Institute of Shanghai Aerospace Control Technology, Shanghai, 200240, P. R. China
zhongchao0327@163.com

Abstract. In this paper, the rest-to-rest reorientation problem of the uncertain spacecraft in the presence of multiple attitude constrained zones and angular velocity limitations is studied. In order to deal with attitude constrained zones and angular velocity limitations concurrently, two types logarithmic potential functions are proposed, where the ineffective attitude constraints are excluded in the design of attitude potential function by introducing a warning angle. In addition, we also designed a projection operator-based adaptive law to estimate the upper bounds of the environmental disturbances and the inertia uncertain parameters, so that the estimation process conforms to the physical meaning of the parameters. Combining the two potential functions and the parameters adaptation law, an adaptive controller is constructed to asymptotically stabilize the attitude reorientation error while satisfying the attitude constraints and the angular velocity limitations. Simulation example of an uncertain rigid spacecraft with rest-to-rest attitude maneuver subject to constraints on attitude and angular velocity is carried out, and the obtained results verify the effectiveness of the proposed adaptive attitude controller.

Keywords: inertia uncertainty, attitude constraint, angular velocity constraint

1 Introduction

The spacecraft attitude control is to reorientate the spacecraft to a desired orientation. Continuous efforts have been made to improve the performance and autonomy of the spacecraft attitude control, such as inverse optimal control

[3] The corresponding author is Shufan Wu.
This work is supported by
1) National Natural Science Foundation of China under Grant, U20B2054.
2) Natural Science Foundation of Shanghai under Grant, 20ZR1427000.
3) Shanghai Sailing Program under Grant, 20YF1421600.
4) SAST-SJTU advanced space technology joint research fund, USCAST2019-22.

[1], adaptive control [2], fuzzy adaptive control [3], backstepping control [4], integral-type sliding mode control [5], nonlinear model predictive control [6] and others. To improve the safety and maneuverability, large angle reorientation under attitude and angular velocity constraints as well as inertia uncertainties has been extensively studied recently.

The scientific spacecraft is often equipped with light-sensitive payloads, such as telescope and interferometer, which are required to change its pointing direction while keeping away from exposing to bright celestials. There are two main methods for solving this constrained attitude control problem, i.e., path planning-based method and potential function-based method. Since path planning-based strategies [7] have complex structure and expensive computation, it is not conducive to spaceborne calculation. In contrast, the potential function-based method incorporate the negative gradient of artificial potential into the controller design, resulting in an analytic attitude controller that is suitable for real-time on-board computation. In [8], a Gaussian function-based potential function was used for spacecraft attitude controller design. In [9], Lee constructed a convex logarithmic-type potential function, with which an attitude controller that guarantees asymptotic error convergence and satisfies attitude constraints result from attitude forbidden and mandatory regions. In [10], a quadratic potential function was proposed to parametrize attitude-constrained zones. In [11], taking the pointing direction deviation of sensitive equipment into account, a robust logarithmic potential function was utilized to design a virtual attitude controller while avoiding attitude-constrained zones.

Another practical constraint in spacecraft attitude controller design is the pre-defined bound of angular velocity determined by performance requirement or saturation limit of rate gyros. To satisfy the angular velocity constraint, Wie developed a cascade quaternion feedback controller for large angle slew problem by using saturation functions [12], whereas the stability analysis was not provided. In [13], a nonlinear attitude controller combined with a control allocation scheme was proposed to achieve attitude stabilization despite actuator saturation limitation and angular velocity constraints. In [14], a bounded adaptive controller was designed to achieve attitude stabilization of spacecraft subject to angular rate constraint, where the neural network approximation and command filter accounting for actuator saturation compensation and the assigned angular velocity respectively are utilized. In [15], the fault-tolerant attitude tracking problem was studied when there are actuator failures and angular velocity constraints in controller design. In [16], Shen presented an adaptive controller to solve the constrained rigid body reorientation problem, where multiple attitude-constrained zones and angular rate limits are taken into account. However, the aforementioned methods do not consider the spacecraft inertia uncertainty, which may deteriorates the control performance.

In this paper, we proposed an adaptive attitude controller to achieve asymptotic redirection for inertia uncertain spacecraft in the presence of attitude-constrained zones and angular velocity constraints. First, two logarithmic potential functions are constructed to describe potential fields of attitude con-

straints and angular velocity limitations, respectively. Then, an adaptive attitude controller considering inertia uncertainty is designed to stabilize the spacecraft asymptotically. Finally, the effectiveness of the proposed adaptive attitude controller is verifed by using numerical simulation of a rest-to-rest attitude maneuver. The main contributions of this paper are summarized as follows:

(1) In contrast to the existing potential function-based attitude controllers [8–10, 16], the proposed adaptive controller can not only satisfy the attitude and angular velocity constraints, but also deal with the inertia uncertainty and external disturbances of spacecraft, thus improving the performance of the controller.
(2) The warning angle is introduced into the attitude potential function design, which can speed up the convergence rate of the error.
(3) The proposed adaptive controller uses a smooth projection operator to design the adaptation law for inertia uncertainty and external disturbances, making the estimated parameters closer to their physical values.

2 Preliminaries

2.1 Spacecraft Dynamic Model

The attitude of spacecraft is described by unit quaternion given by

$$\mathbb{Q}_u = \{\boldsymbol{Q} = \left[\boldsymbol{q}^T, q_0\right]^T \in \mathbb{R}^3 \times \mathbb{R} \mid \boldsymbol{q}^T\boldsymbol{q} + q_0^2 = 1\}, \tag{1}$$

where $\boldsymbol{q} \in \mathbb{R}^3$ and $q_0 \in \mathbb{R}$ represent the vector part and scalar part, respectively. Let $\boldsymbol{Q}_d \in \mathbb{Q}_u$ denote the desired attitude. The unit-quaternion error $\boldsymbol{Q}_e = [q_{e1}, q_{e2}, q_{e3}, q_{e0}]^T = \left[\boldsymbol{q}_e^T, q_{e0}\right]^T \in \mathbb{Q}_u$ can be obtained as $\boldsymbol{Q}_e = \boldsymbol{Q}_d^* \odot \boldsymbol{Q} = \left[\boldsymbol{q}_e^T, q_{e0}\right]^T$, where $\odot$ is the quaternion multiplication operator, and quaternion conjugate or inverse is defined as $\boldsymbol{Q}^* = \left[-\boldsymbol{q}^T, q_0\right]^T$. Moreover, we denote $\boldsymbol{\omega}_d$ as the desired angular velocity in the desired reference frame $\mathcal{N}$. Note that this paper focuses on the rest-to-rest reorientation control, and hence $\boldsymbol{\omega}_d = 0$.

Then, the kinematics and dynamics of the spacecraft with inertial uncertainty can be described as [17]:

$$\dot{\boldsymbol{Q}}_e = \frac{1}{2}\begin{bmatrix}\boldsymbol{S}\left(\boldsymbol{q}_e\right) + q_{e0}\boldsymbol{I}_3 \\ -\boldsymbol{q}_e^T\end{bmatrix}\boldsymbol{\omega} \tag{2}$$

$$\boldsymbol{J}\dot{\boldsymbol{\omega}} = -\boldsymbol{S}(\boldsymbol{\omega})\boldsymbol{J}\boldsymbol{\omega} + \boldsymbol{u} + \boldsymbol{d}, \tag{3}$$

where $\boldsymbol{\omega} \in \mathbb{R}^3$ is the angular velocity of the spacecraft in the body frame $\mathcal{B}$ with respect to an inertial frame $\mathcal{I}$, the matrix $\boldsymbol{S}(\boldsymbol{x}) \in \mathbb{R}^{3\times3}$ denotes a skew-symmetric matrix, $\boldsymbol{u} \in \mathbb{R}^3$ is the resultant control torque acting on the spacecraft, the environmental disturbance is denoted as $\boldsymbol{d} \in \mathbb{R}^3$.

Assumption 1 *The external disturbance* $\boldsymbol{d}$ *is assumed to be upper bounded by* $\|\boldsymbol{d}\| \leq d_{\max}$ *with* $d_{\max}$ *being a positive scalar, and* $\|*\|$ *is the Euclidean norm.*

The uncertain inertia matrix $\boldsymbol{J} \in \mathbb{R}^{3\times 3}$ of the spacecraft is decomposed as

$$\boldsymbol{J} = \boldsymbol{J}_0 + \boldsymbol{J}_1, \tag{4}$$

where $\boldsymbol{J}_0$ and $\boldsymbol{J}_1$ denote the nominal/known part and unknown part of the inertia $\boldsymbol{J}$, respectively. Here, we also assume that $\boldsymbol{J}_1$ is bounded, i.e, $\|\boldsymbol{J}_1\| \leq J_{1,max}$. Then, the dynamics in (3) can be further written as

$$\boldsymbol{J}_0\dot{\boldsymbol{\omega}} = -\boldsymbol{S}(\boldsymbol{\omega})\boldsymbol{J}_0\boldsymbol{\omega} + \boldsymbol{u} + \boldsymbol{d} - \boldsymbol{J}_1\dot{\boldsymbol{\omega}} - \boldsymbol{S}(\boldsymbol{\omega})\boldsymbol{J}_1\boldsymbol{\omega}. \tag{5}$$

Motived by [17], the following lemma is developed:

Lemma 1. *The nonlinear term* $\boldsymbol{d} - \boldsymbol{J}_1\dot{\boldsymbol{\omega}} - \boldsymbol{S}(\boldsymbol{\omega})\boldsymbol{J}_1\boldsymbol{\omega}$ *in* (5) *satisfies*

$$\|\boldsymbol{d} - \boldsymbol{J}_1\dot{\boldsymbol{\omega}} - \boldsymbol{S}(\boldsymbol{\omega})\boldsymbol{J}_1\boldsymbol{\omega}\| \leq Dh(\boldsymbol{q}_e, \boldsymbol{\omega}), \tag{6}$$

where the scalar $D \triangleq \max(\|\boldsymbol{d}\| + D_0\|\boldsymbol{J}_1\|, (D_0 + r_4)\|\boldsymbol{J}_1\|)$ *being an unknown positive constant satisfies* $\|D\| \leq D_{\max}$*, and* $h(\boldsymbol{q}_e, \boldsymbol{\omega}) = 1 + \|\boldsymbol{q}_e\| + \|\boldsymbol{\omega}\| + \|\boldsymbol{\omega}\|^2$.

Proof. According to the kinematics (2) and dynamics (3), $\dot{\boldsymbol{\omega}}$ can be expressed as a function of $\boldsymbol{q}_e$, $\boldsymbol{\omega}$ and $\boldsymbol{u}$, i.e, $\dot{\boldsymbol{\omega}} = f(\boldsymbol{q}_e, \boldsymbol{\omega}, \boldsymbol{u})$. Since $\boldsymbol{u}$ can be expressed as $\boldsymbol{u} = g(\boldsymbol{q}_e, \boldsymbol{\omega})$, we have

$$\dot{\boldsymbol{\omega}} = f(\boldsymbol{q}_e, \boldsymbol{\omega}, g(\boldsymbol{q}_e, \boldsymbol{\omega})).$$

Assuming that the function f is linear with respect to $\boldsymbol{q}_e$, $\boldsymbol{\omega}$, $\boldsymbol{\omega}^T\boldsymbol{\omega}$, then taking Euclidean norm on both sides of the above equation yields

$$\begin{aligned}\|\dot{\boldsymbol{\omega}}\| &\leq r_0\|\boldsymbol{\omega}\| + r_1\|\boldsymbol{\omega}\|^2 + r_2\|\boldsymbol{q}_e\| + r_3\\ &\leq D_0(1 + \|\boldsymbol{q}_e\| + \|\boldsymbol{\omega}\| + \|\boldsymbol{\omega}\|^2),\end{aligned}$$

where r_0, r_1, r_2 and r_3 are unknown positive constant, $D_0 = \max(r_0, r_1, r_2, r_3)$. Consequently, the following inequality holds:

$$\begin{aligned}\|\boldsymbol{d} - \boldsymbol{J}_1\dot{\boldsymbol{\omega}} - \boldsymbol{S}(\boldsymbol{\omega})\boldsymbol{J}_1\boldsymbol{\omega}\| &\leq \|\boldsymbol{d}\| + \|\boldsymbol{J}_1\|\|\dot{\boldsymbol{\omega}}\| + r_4\|\boldsymbol{J}_1\|\|\boldsymbol{\omega}\|^2\\ &\leq \|\boldsymbol{d}\| + D_0\|\boldsymbol{J}_1\|(1 + \|\boldsymbol{q}_e\| + \|\boldsymbol{\omega}\| + \|\boldsymbol{\omega}\|^2) + r_4\|\boldsymbol{J}_1\|\|\boldsymbol{\omega}\|^2\\ &\leq \|\boldsymbol{d}\| + D_0\|\boldsymbol{J}_1\| + D_0\|\boldsymbol{J}_1\|\|\boldsymbol{q}_e\| + D_0\|\boldsymbol{J}_1\|\|\boldsymbol{\omega}\| + (D_0 + r_4)\|\boldsymbol{J}_1\|\|\boldsymbol{\omega}\|^2\\ &\leq Dh(\boldsymbol{q}_e, \boldsymbol{\omega}),\end{aligned}$$

where $D \triangleq \max(\|\boldsymbol{d}\| + D_0\|\boldsymbol{J}_1\|, (D_0 + r_4)\|\boldsymbol{J}_1\|)$.

Since the unknown positive constant r_4, $\|\boldsymbol{d}\|$ and $\|\boldsymbol{J}_1\|$ are bounded, the unknown positive constant D can be assumed to satisfy $\|D\| \leq D_{\max}$ with $D_{\max}$ being an unknown positive constant.

2.2 Attitude Constrained Zones

Definition 1 (Attitude-Constrained Zone [9]). *The attitude-constrained zone is defined as the set of attitudes that spaceborne sensitive instrument (e.g., infrared telescopes or optical instruments) directly exposes to certain celestial objects (e.g., the sun). Multiple constrained zones can be specified with respect to a single spaceborne equipment boresight vector.*

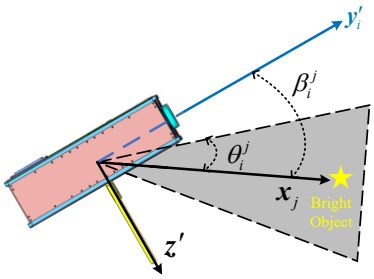

Fig. 1: Demonstration of attitude constrained zone.

Supposing that the pointing direction of sensitive instrument is expressed as $\boldsymbol{y}_i$ in the body frame $\mathcal{B}$, the corresponding pointing direction is the inertial frame $\mathcal{I}$ is derived by

$$\boldsymbol{y}_i' = \boldsymbol{Q} \odot \boldsymbol{y}_i \odot \boldsymbol{Q}^* = \boldsymbol{y}_i - 2(\boldsymbol{q}^T\boldsymbol{q})\boldsymbol{y}_i + 2(\boldsymbol{q}^T\boldsymbol{y}_i)\boldsymbol{q} + 2q_0(\boldsymbol{y}_i \times \boldsymbol{q}). \tag{7}$$

As depicted in Fig. 1, $\boldsymbol{x}_j$ is the normalized vector pointing toward a certain bright object in the inertial frame $\mathcal{I}$. In order to avoid direct exposure to the bright object, the angle between the $\boldsymbol{y}_i'$ and $\boldsymbol{x}_j$ (i.e., β_i^j) is required to be strictly greater than θ_i^j. That is, the constraint $\beta_i^j > \theta_i^j$ with $0 < \theta_i^j < \pi$ should be maintained, which can be formulated as

$$\boldsymbol{x}_j \cdot \boldsymbol{y}_i' < \cos(\theta_i^j). \tag{8}$$

Substituting (7) into (8) leads to

$$2\boldsymbol{q}^T\boldsymbol{y}_i\boldsymbol{q}^T\boldsymbol{x}_j - \boldsymbol{q}^T\boldsymbol{q}\boldsymbol{x}_j^T\boldsymbol{y}_i + q_0^2\boldsymbol{x}_j^T\boldsymbol{y}_i + 2q_0\boldsymbol{q}^T(\boldsymbol{x}_j \times \boldsymbol{y}_i) < \cos(\theta_i^j). \tag{9}$$

Then, the constraint (9) can be further written as [9]

$$\boldsymbol{Q}^T\boldsymbol{M}_i^j\boldsymbol{Q} < 0, \tag{10}$$

where the matrix $\boldsymbol{M}_i^j$ associated with the j-th celestial object and the i-th sensitive equipment ($i = 1, \ldots, n$ and $j = 1, \ldots, m$) is defined as

$$\begin{aligned} \boldsymbol{M}_i^j &= \begin{bmatrix} \boldsymbol{A}_i^j & \boldsymbol{b}_i^j \\ \boldsymbol{b}_i^{jT} & d_i^j \end{bmatrix}, \boldsymbol{b}_i^j = \boldsymbol{x}_j \times \boldsymbol{y}_i, d_i^j = \boldsymbol{x}_j^T\boldsymbol{y}_i - \cos(\theta_i^j), \\ \boldsymbol{A}_i^j &= \boldsymbol{x}_j\boldsymbol{y}_i^T + \boldsymbol{y}_i\boldsymbol{x}_j^T - \left(\boldsymbol{x}_j^T\boldsymbol{y}_i + \cos(\theta_i^j)\right)\boldsymbol{I}_3. \end{aligned} \tag{11}$$

As a consequence, the set of attitudes $\boldsymbol{Q}_{F_i^j} \subseteq \mathbb{Q}_u$ that are outside of the j-th attitude constrained zone for the i-th sensitive instrument can be described as

$$\boldsymbol{Q}_{F_i^j} = \left\{\boldsymbol{Q} \in \mathbb{Q}_u \mid \boldsymbol{Q}^T\boldsymbol{M}_i^j(\theta_i^j)\boldsymbol{Q} < 0\right\}. \tag{12}$$

Generally, we need to take into consideration the attitude-constrained zones that are related to all n spaceborne sensitive instruments and their associated m bright objects.

In addition, the concept of warning angle is introduced to specify the necessary attitude-constrained zones that are to be considered in the potential function design.

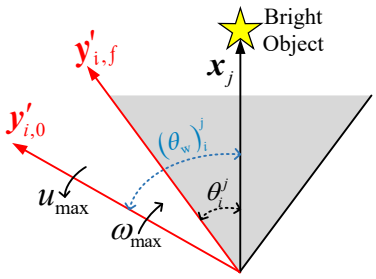

Fig. 2: Demonstration of warning angle.

As shown in Fig. 2, the warning angle inspired by [11] can be obtained as

$$(\theta_w)_i^j = \frac{1}{2}\frac{J_{\max}}{u_{\max}}\omega_{\max}^2 + \theta_i^j, \tag{13}$$

where $J_{\max}$ is the inertia of the major principal axis, $u_{\max}$ is the maximum torque acted to decelerate the spacecraft, $\omega_{\max}$ is the maximum angular velocity.

Remark 1. The defined warning angle helps to exclude the ineffective attitude constraints in the potential function design. To be more specific, if the angle between the pointing direction vector $\boldsymbol{y}_i'$ and the normalized vector $\boldsymbol{x}_j$ pointing toward a certain bright object is greater than the warning angle, i.e., $\beta_i^j > (\theta_w)_i^j$, the influence of the j-th attitude constrained zone to the i-th spaceborne sensitive equipment can be ignored in the construction of the potential field.

2.3 Angular Velocity Constraints

In practical spacecraft missions, angular velocity constraints may be required as a result of the limited measurement range of the rate gyroscopes or scientific mission requirements. The set of allowable angular velocity is expressed as

$$\boldsymbol{W} = \left\{\boldsymbol{\omega} \in \mathbb{R}^3 \middle| |\omega_i| \leq \omega_{i,\max}\right\}, \tag{14}$$

where $\omega_{i,\max}(i = 1, 2, 3)$ is the limitation of allowable angular velocity for each axis.

3 Problem Statement

The schematic diagram of the overall attitude control system is depicted in Fig. 3, where two problems are to be solved in this paper:

Problem 1. [Potential function] In view of the warning angle, design potential functions for the attitude constraints and angular velocity constraints.

Problem 2. [Adaptive Control] Leveraging the proposed potential functions, design an adaptive attitude controller with the projection operator in the adaptive law to achieve asymptotic attitude control despite the presence of the attitude and angular velocity constraints.

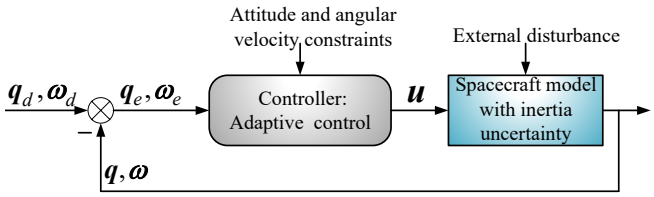

Fig. 3: The overall schematic diagram of the spacecraft attitude control system.

4 Potential Function Design

We solve the Problem 1 in this section, where two logarithmic potential functions are proposed for attitude constraints and angular velocity limitations, respectively.

4.1 Potential Function for Attitude-Constrained Zones

For the attitude constrained zones, a logarithmic potential function $V_1(\boldsymbol{Q}) : \boldsymbol{Q}_p \to \mathbb{Q}_u$ is proposed as

$$V_1(\boldsymbol{Q}) = \|\boldsymbol{Q}_d - \boldsymbol{Q}\|^2 \left[\sum_{j=1}^{m} \sum_{i=1}^{n} -\alpha k_{ij} \log \left(- \frac{\boldsymbol{Q}^T \boldsymbol{M}_i^j(\theta_i^j) \boldsymbol{Q}}{2} \right) \right] \tag{15}$$

where α is a positive weighting constant, and the parameter k_{ij} relating to the warning angle is defined as

$$k_{ij} = \begin{cases} 0, & \text{if } \beta_i^j > \theta_i^j \\ 1, & \text{if } \beta_i^j \leq \theta_i^j \end{cases} \tag{16}$$

Remark 2. Compared with the existing potential function proposed in [11], the proposed one in (15) considers the effects of the warning angle. When the i-th spaceborne sensitive equipment points away from the corresponding j-th constrained zone, according to Remark 1, the j-th constrained zone can be ignore, i.e., $k_{ij} = 0$. As a result, the unnecessary constrained zones are not taken into account in the potential function design.

Lemma 2 (Proposition 6 in [9]).
The potential function $V_1(\boldsymbol{Q})$ meets the following three conditions:

- $V_1(\boldsymbol{Q}_d) = 0$;
- $V(\boldsymbol{Q}) > 0$, *for all* $\boldsymbol{Q} \in \boldsymbol{Q}_p \backslash \{\boldsymbol{Q}_d\}$;
- $\nabla^2 V(\boldsymbol{Q}) > 0$ *is positive definite for all* $\boldsymbol{Q} \in \boldsymbol{Q}_p$.

4.2 Potential Function for Angular Velocity Constraint

In addition, to incorporate the angular velocity constraints defined in (14) in attitude controller design, a logarithmic potential function V_2 is designed as

$$V_2(\boldsymbol{\omega}) = \frac{1}{2}\sum_{i=1}^{3} \log\left(\frac{\omega_{i,\max}^2}{\omega_{i,\max}^2 - \omega_i^2}\right). \tag{17}$$

The above potential function satisfies the following lemma:

Lemma 3. *The potential function $V_2(\boldsymbol{\omega})$ has the following three properties:*

- $V_2(0) = 0$;
- $V_2(\boldsymbol{\omega}) > 0$, *for all* $\boldsymbol{\omega} \in \boldsymbol{W} \backslash \{0\}$;
- $\nabla^2 V_2(\boldsymbol{\omega}) > 0$ *is positive for all* $\boldsymbol{\omega} \in \boldsymbol{W}$.

Proof. Based on the defined logarithmic potential function $V_2(\boldsymbol{\omega})$, it is trivial to verify that $V_2(0) = 0$. In addition, the following inequality

$$\frac{\omega_{i,\max}^2}{\omega_{i,\max}^2 - \omega_i^2} > 1 \tag{18}$$

holds for all $\boldsymbol{\omega} \in \boldsymbol{W} \backslash \{0\}$, which subsequently yields

$$\log\left(\frac{\omega_{i,\max}^2}{\omega_{i,\max}^2 - \omega_i^2}\right) > 0, \tag{19}$$

hence, $V_2(\boldsymbol{\omega}) > 0$, for all $\boldsymbol{\omega} \in \boldsymbol{W} \backslash \{0\}$.

As the third property of Lemma 3, due to the fact that the three terms in the potential function $V_2(\boldsymbol{\omega})$ are independent, it is sufficient to only have a detailed analysis to one of the three terms. Taking ω_1 as an example, we have

$$V_2(\omega_1) = \log\left(\frac{\omega_{1,\max}^2}{\omega_{1,\max}^2 - \omega_1^2}\right). \tag{20}$$

The gradient of $V_2(\omega_1)$ can be calculated as

$$\nabla V_2(\omega_1) = \frac{\omega_1}{\omega_{1,\max}^2 - \omega_1^2}. \tag{21}$$

Consequently, the Hessian $\nabla^2 V_2(\omega_1)$ can be given as

$$\nabla^2 V_2(\omega_1) = \frac{\omega_{1,\max}^2 + \omega_1^2}{(\omega_{1,\max}^2 - \omega_1^2)^2} > 0. \tag{22}$$

Therefore, it is clear that $\nabla^2 V_2(\boldsymbol{\omega}) > 0$ if $\boldsymbol{\omega} \in \boldsymbol{W}$.

5 Adaptive Controller Design

In this section, the Problem 2 is solved by leveraging the proposed potential functions, leading to an adaptive attitude controller that realize the spacecraft attitude redirection in the presence of inertia uncertainty. The adaptive controller is designed as

$$\begin{aligned}\boldsymbol{u} =& \boldsymbol{S}(\boldsymbol{\omega})\boldsymbol{J}_0\boldsymbol{\omega} - k_1\boldsymbol{q}_e^T\boldsymbol{q}_e\boldsymbol{\Phi}\frac{\tanh(\boldsymbol{\omega})}{\|\boldsymbol{\omega}\|} - k_2\boldsymbol{\Phi}\boldsymbol{\omega} - 2k_3\boldsymbol{\Phi}\boldsymbol{q}_e \\ &+ k_4\boldsymbol{\Phi}\mathrm{Vec}[(\nabla V_1^* \odot \boldsymbol{Q})] - \hat{D}_{\max}h(\boldsymbol{\omega},\boldsymbol{q}_e)\tanh(\boldsymbol{\Phi}^{-1}\boldsymbol{\omega})\end{aligned} \tag{23}$$

where $\boldsymbol{\Phi} = \boldsymbol{\lambda}\boldsymbol{J}_0^{-1}$ with $\boldsymbol{\lambda} = \mathrm{diag}\{(\omega_{1,\max}^2 - \omega_1^2), (\omega_{2,\max}^2 - \omega_2^2), (\omega_{3,\max}^2 - \omega_3^2)\}$, and k_1, k_2 and k_3 are positive constants, $\hat{D}_{\max}$ is the estimate of the unknown scalar $D_{\max}$ in Lemma 1.

To construct the adaptive law for $\hat{D}_{\max}$, we assume that the unknown scalar $D_{\max}$ for $\boldsymbol{D}$ is also bounded. Define two convex sets as

$$\begin{aligned}\Omega_{D_{\max}} &\triangleq \left\{D_{\max} \in \mathbb{R} \mid D_{\max}^2 < \epsilon\right\}, \\ \Omega_{\hat{D}_{\max}} &\triangleq \left\{\hat{D}_{\max} \in \mathbb{R} \mid \hat{D}_{\max}^2 < \epsilon + \delta\right\},\end{aligned} \tag{24}$$

where $\epsilon > 0$ and $\delta > 0$ are two known constants. The updating scheme for $\hat{D}_{\max}$ is given by

$$\dot{\hat{D}}_{\max} = \mathrm{Proj}(\hat{D}_{\max}, \Psi), \quad \Psi \triangleq h(\boldsymbol{\omega},\boldsymbol{q}_e)\|\boldsymbol{\Phi}^{-1}\boldsymbol{\omega}\|, \tag{25}$$

where the projection operator is constructed as

$$\mathrm{Proj}(\hat{D}_{\max}, \Psi) \triangleq \begin{cases} r\Psi, & \text{if } \hat{D}_{\max}^2 < \epsilon \\ r(\Psi - \frac{(\hat{D}_{\max}^2 - \epsilon)\Psi\hat{D}_{\max}}{\delta\hat{D}_{\max}^2}\hat{D}_{\max}), & \text{if } \hat{D}_{\max}^2 \geq \epsilon \end{cases} \tag{26}$$

where r is a positive constant. The above parameter updating law is locally Lipschitz continuous and guarantees that the estimate $\hat{D}_{\max}$ is always within the convex set defined in (24), i.e., $\hat{D}_{\max} \in \Omega_{\hat{D}_{\max}}$ if $\hat{D}_{\max}(0) \in \Omega_{\hat{D}_{\max}}$.

The stability of the closed-loop attitude control system is summarized as follows:

Theorem 1. *Consider the attitude kinematics and dynamics of an inertia uncertain spacecraft, as modeled in* (2) *and* (5)*. The potential function-based attitude controller in* (23) *combined with an adaptive law in* (25) *solves the Problem 2, so that* $\lim_{t\to\infty}\boldsymbol{q}_e(t) = 0$ *and* $\lim_{t\to\infty}\boldsymbol{\omega}(t) = 0$ *and that attitude and angular velocity constraints are satisfied.*

Proof. Choose the following Lyapunov candidate:

$$V = 2k_3(\boldsymbol{q}_e{}^T\boldsymbol{q}_e + (1 - q_{e0})^2) + 2k_4V_1 + V_2 + V_D, \tag{27}$$

where $V_D = \frac{1}{2r}\tilde{D}_{\max}^2$, and $\tilde{D}_{\max} = \hat{D}_{\max} - D_{\max}$ is the estimation error of the $D_{\max}$. Taking time derivative of V leads to

$$\dot{V} = 2k_3 \boldsymbol{q}_e{}^T \boldsymbol{\omega} + 2k_4 \nabla V_1^T [\frac{1}{2}\boldsymbol{Q} \otimes \boldsymbol{v}(\boldsymbol{\omega})] + \boldsymbol{\omega}^T \boldsymbol{\Phi}^{-1} \boldsymbol{J}_0 \dot{\boldsymbol{\omega}} + \frac{1}{r}\tilde{D}_{\max}\dot{\tilde{D}}_{\max}. \tag{28}$$

Then, in light of $k_3 \nabla V_1^T [\boldsymbol{Q} \otimes \boldsymbol{v}(\boldsymbol{\omega})] = -k_3 \boldsymbol{\omega}^T \mathrm{Vec}[\nabla V_1^* \otimes \boldsymbol{Q}]$, substituting the adaptive controller defined in (23) and adaptive law designed in (25) into the foregoing equation yields

$$\begin{aligned}\dot{V} =& 2k_3 \boldsymbol{q}_e{}^T \boldsymbol{\omega} - k_4 \boldsymbol{\omega}^T \mathrm{Vec}[\nabla V_1^* \otimes \boldsymbol{Q}] + \frac{1}{r}\tilde{D}_{\max}\dot{\tilde{D}}_{\max} \\ &+ \boldsymbol{\omega}^T \boldsymbol{\Phi}^{-1}\big(- k_1 \boldsymbol{q}_e^T \boldsymbol{q}_e \boldsymbol{\Phi} \frac{\tanh(\boldsymbol{\omega})}{\|\boldsymbol{\omega}\|} - k_2 \boldsymbol{\Phi}\boldsymbol{\omega} + k_4 \boldsymbol{\Phi}\mathrm{Vec}[(\nabla V_1^* \otimes \boldsymbol{Q})] \\ &- 2k_3 \boldsymbol{\Phi}\boldsymbol{q}_e - \hat{D}_{\max} h(\boldsymbol{\omega}) \tanh(\boldsymbol{\Phi}^{-1}\boldsymbol{\omega}) + \boldsymbol{d} - \boldsymbol{J}_1 \dot{\boldsymbol{\omega}} - \boldsymbol{S}(\boldsymbol{\omega})\boldsymbol{J}_1\boldsymbol{\omega}\big),\end{aligned} \tag{29}$$

By substituting (6) further research can be obtained

$$\begin{aligned}\dot{V} \leq& - k_1 \|\boldsymbol{q}_e\|^2 - k_2 \|\boldsymbol{\omega}\|^2 - \tilde{D}_{\max} h(\boldsymbol{\omega}, \boldsymbol{q}_e) \big\|\boldsymbol{\Phi}^{-1}\boldsymbol{\omega}\big\| + \frac{1}{r}\tilde{D}_{\max}\dot{\tilde{D}}_{\max} \\ \leq& - k_1 \|\boldsymbol{q}_e\|^2 - k_2 \|\boldsymbol{\omega}\|^2 + \frac{1}{r}\tilde{D}_{\max}(\dot{\hat{D}}_{\max} - r h(\boldsymbol{\omega}, \boldsymbol{q}_e)\big\|\boldsymbol{\Phi}^{-1}\boldsymbol{\omega}\big\|) \\ \leq& - k_1 \|\boldsymbol{q}_e\|^2 - k_2 \|\boldsymbol{\omega}\|^2 + \frac{1}{r}\tilde{D}_{\max}(\dot{\hat{D}}_{\max} - r\Psi)\end{aligned} \tag{30}$$

which is negative semi-definite if

$$\tfrac{1}{r}\tilde{D}_{\max}\left(\dot{\hat{D}}_{\max} - r\Psi\right) \leq 0. \tag{31}$$

According to the adaptive updating law of $\hat{D}_{\max}$ in (25), $\frac{1}{r}\tilde{D}_{\max}\left(\dot{\hat{D}}_{\max} - r\Psi\right) \leq= 0$ if $\|\hat{D}_{\max}\|^2 < \epsilon$. Furthermore, if $\|\hat{D}_{\max}\|^2 \geq \epsilon$ and $\Psi\hat{D}_{\max} > 0$, then we have

$$\begin{aligned}\frac{1}{r}\tilde{D}_{\max}(\dot{\hat{D}}_{\max} - r\Psi) &= \frac{1}{r}\tilde{D}_{\max}(r(\Psi - \frac{(\hat{D}_{\max}^2 - \epsilon)\Psi\hat{D}_{\max}}{\delta\hat{D}_{\max}^2}\hat{D}_{\max}) - r\Psi) \\ &= -(\frac{(\hat{D}_{\max}^2 - \epsilon)\Psi\hat{D}_{\max}}{\delta\hat{D}_{\max}^2}\tilde{D}_{\max}\hat{D}_{\max}) \leq 0\end{aligned} \tag{32}$$

Since $\tilde{D}_{\max}\hat{D}_{\max} = \hat{D}_{\max}^2 - D_{\max}\hat{D}_{\max} \geq 0$ when $\hat{D}_{\max}^2 \geq \epsilon$. Therefore, we have the result that (31) is satisfied by using the proposed adaptive law. Therefore, we have that $\dot{V}$ satisfies

$$\dot{V} \leq - k_1 \|\boldsymbol{q}_e\|^2 - k_2 \|\boldsymbol{\omega}\|^2 \leq 0. \tag{33}$$

Consequently, by invoking Barbalat's Lemma [19], it is clear that $\lim_{t\to\infty} \boldsymbol{q}_e(t) = 0$ and $\lim_{t\to\infty} \boldsymbol{\omega}(t) = 0$.

Remark 3. Note that in (23), the term of the positive scalars k_1 and k_3 are related to the attitude convergence rate, when their values are increased, the attitude convergence speed will be accelerated, but excessive angular velocity cause the sensitive equipment to enter the attitude constrained zones. The scalars k_2 and k_4 are analogous to the damping terms. When the angular velocity increases, the degree of damping increase, making the state trajectory smoother. In addition, k_4 represents the influence of the attitude-constrained zones. When k_4 becomes larger, it is easier to avoid the attitude-constrained zones.

6 Simulation Results

The nominal part inertia of spacecraft is

$$\boldsymbol{J}_0 = \begin{bmatrix} 20 & 0 & 0 \\ 0 & 15 & 0 \\ 0 & 0 & 20 \end{bmatrix} \text{kg} \cdot \text{m}^2,$$

and unknown part is set to $\boldsymbol{J}_1 = 0.1\boldsymbol{J}_0$. The environmental disturbance is assumed to be

$$\boldsymbol{d} = 10^{-2} \begin{bmatrix} -1 + 3\sin(0.1t + \pi/2) + 4\sin(0.03t) \\ 1.5 - 1.5\sin(0.02t) - 3\sin(0.05t + \pi/2) \\ 1 + 2\sin(0.1t) - 1.5\sin(0.04t + \pi/2) \end{bmatrix} \text{N} \cdot \text{m}$$

The reaction wheels are installed on the x, y, z axes of the spacecraft body coordinate frame $\mathcal{B}$ and are limited by $|\tau_i| \leq 0.25$ N·m for $i \in \{1, 2, 3\}$. As a result, the output torque needs to satisfy $\|\boldsymbol{u}\| \leq 0.433$ N·m. Moreover, the maximal angular velocity about each axis is set to be 6 deg/s, i.e., $\|\boldsymbol{\omega}\| \leq 10.4$ deg/s.

In the simulation, the spacecraft is equipped a sensitive instrument, whose boresight vector is along the spacecraft body axis $\boldsymbol{y}$. Four attitude constrained zones, which do not overlap with each other, are considered and their details can be found in Table 1. Here, the Initial attitude is assumed to be $\boldsymbol{Q}(0) = [-0.352, 0.12, 0, 0.9284]^T$ and initial angular velocity is set to be $\boldsymbol{\omega}(0) = [0, 0, 0]^T$ deg/s, The desired attitude is $\boldsymbol{Q}_d = [0.7024, 0.6790, 0, 0.2133]^T$, which is chosen to be outside of four attitude forbidden zones. According to (13), the corresponding warning angles of 4 constrained zones can be obtained as $(\theta_w)_1^1 = 73.6$ deg, $(\theta_w)_1^2 = 63.6$ deg, $(\theta_w)_1^3 = 68.6$ deg and $(\theta_w)_1^4 = 73.6$ deg.

Table 1: Parameters of attitude constraints

Constrained zones	Center vector (inertial frame)	Angle, deg
Zone 1 (CZ1)	[0;-1;0]	30
Zone 2 (CZ3)	[0.68;0.67;0.28]	20
Zone 3 (CZ3)	[0.38;0;0.925]	25
Zone 4 (CZ4)	[-0.813;0.548;-0.192]	30

6.1 Overall Simulation Result

In this subsection, the overall attitude control result under the proposed controller is given. The controller parameters is given in Table 2.

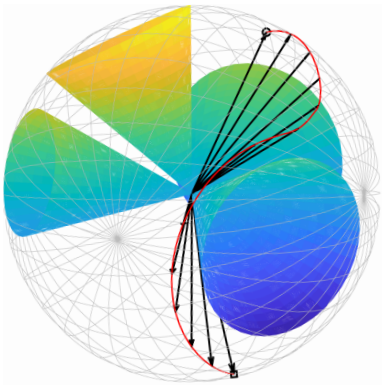

(a) Motion trajectory of sensitive equipment in 3-D

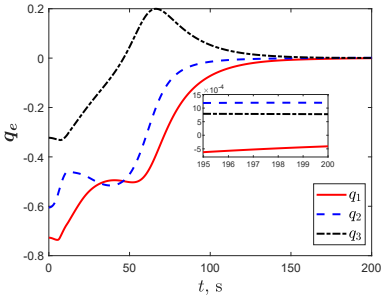

(b) Attitude error vecter $\boldsymbol{q}_e$

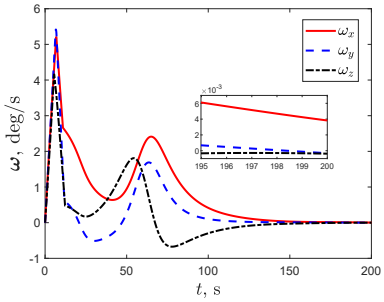

(c) Angular velocity vecter $\boldsymbol{\omega}$

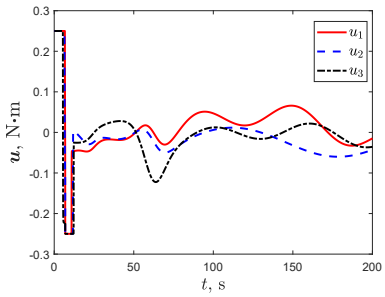

(d) Actuator output torque $\boldsymbol{u}$

Fig. 4: Time response of the simulation results under the angular velocity limit of 6 deg/s.

The Fig. 4 shows the overall simulation results with angular velocity limits 6 deg/s. The 3-D trajectories of the sensitive spaceborne equipment pointing direction are depicted in Fig. 4a, it is observed that the proposed adaptive controller (23) based on potential functions (15) and (17) avoid all attitude-constrained zones under the condition of angular velocity limitation. It not only protects the sensitive equipment, but also realizes the attitude redirection maneuver.

According to Figs. 4b and 4c, the steady-state attitude error and the angular velocity errors are less than 1.2×10^{-3} and 6×10^{-3} deg/s, respectively. Both the attitude and angular velocity convergence errors show that the proposed attitude controller (23) can effectively handle the inertia parameter uncertainty and external disturbance despite angular velocity limits. Since the controller

output is limited directly in the simulation system, the bang-bang control will appear in the controller output, as shown in Fig. 4d.

As for the estimation of external disturbance and inertial uncertainty, the introduction of projection operator (26) can improve the estimation speed and meet the physical meaning of estimation parameters, as shown in Fig. 5. It is clear that a bigger r only speeds up the estimation without changing the upper bound of the estimated value when other parameters do not change.

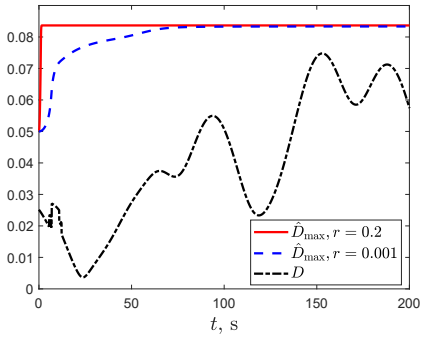

Fig. 5: The time response of the estimate of the unknown parameter $\boldsymbol{D}$.

6.2 Comparison Results

In this subsection, we compare the proposed adaptive controller (23) with existing attitude controllers. For comparison, the controller (58) in [9] and the PD controller in [20] are also implemented. The control gains of three controllers are given in Table 2.

Table 2: Control gains

Control schemes	Control gains
The proposed controller (23)	$k_1 = 0.02$, $k_2 = 120$, $k_3 = 4$, $k_4 = 5$, $\alpha = 0.18$, $r = 0.2$, $\varepsilon = 1.5$, $\delta = 10^{-3}$
Controller (58) in [9]	$\alpha = 160$, $k_1 = 5.4$
PD controller in [20]	$k_p = 20$, $k_d = 100$

The 2-D projection of the pointing direction of sensitive instrument under three controllers are depicted in Fig. 6a. It is observed that trajectories using the PD controller violate attitude constraints, whereas the proposed adaptive controller and the controller (58) in [9] can satisfy attitude constraints.

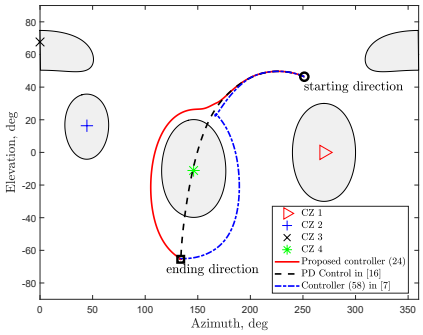

(a) Motion trajectory of sensitive equipment in 2-D under three controllers

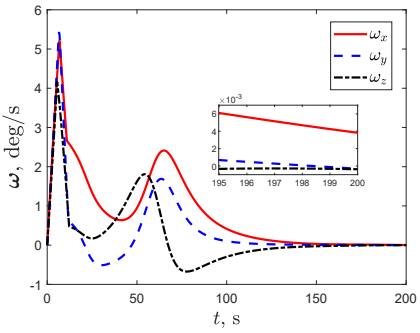

(b) Angular velocity vecter $\boldsymbol{\omega}$ using the proposed controller

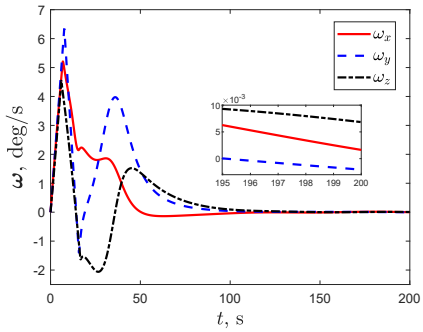

(c) Angular velocity vecter $\boldsymbol{\omega}$ using the controller (58) in [9]

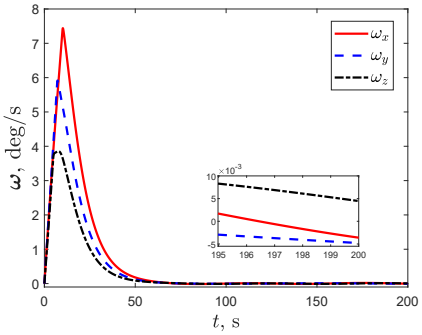

(d) Angular velocity vecter $\boldsymbol{\omega}$ using the PD controller in [20]

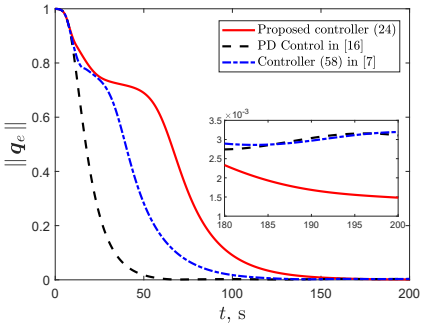

(e) Attitude error $\|\boldsymbol{q}_e\|$ under three controllers

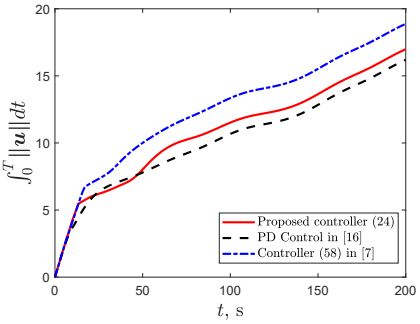

(f) Energy consumption under three controllers

Fig. 6: Simulation results under three controllers.

The angular velocity comparison of the three controllers is presented in Figs. 6b-6d, it is clear that the proposed controller satisfies the angular velocity limit of 6 deg/s, and both other controllers violate the limit value. The attitude error comparison of the three controllers is presented in Fig. 6e. Since the warning angle is considered in the potential function of the proposed controller, its convergence rate is equivalent to that of PD controller at the beginning of simulation, resulting in improved convergence rate when compared with that of the controller (58) in [9] Moreover, the proposed controller (23) considers the inertia uncertainty and external disturbance, so the robustness of the controller and control accuracy of attitude error and angular velocity are higher than that of other two controllers.

In addition, using $\int_0^T \|\boldsymbol{u}\| dt$ (T is the simulation time) to evaluate the overall energy consumption, it is clear from Fig. 6f that the proposed controller and the controller (58) in [9] spend more energy than the PD controller, which is due to the fact that it has to ensure the spaceborne equipment pointing direction meet the attitude constraints. Then, since the controller (58) in [9] does not consider the angular velocity limit, it takes more energy to accelerate and decelerate with a larger angular velocity than the proposed controller.

7 Conclusions

This paper presents a potential function-based adaptive attitude controller to accomplish the attitude redirection for inertia uncertainty spacecraft in the presence of attitude constrained zones and angular velocity limitations. By introducing the concept of warning angle, two kinds of logarithmic potential functions are utilized to deal with the attitude constraint and angular velocity constraint simultaneously. Leveraging the proposed potential functions, we further designed a projection operator-based adaptive law to guarantee that the estimation process conforms to the physical meaning of the estimated parameters. The simulation results demonstrates that the proposed adaptive controller can achieve rest-to-rest attitude redirection despite the presence of inertia uncertainty, external disturbances, angular velocity limitation and multiple attitude-constrained zones.

References

1. Wencheng Luo, Yun-Chung Chu and Keck-Voon Ling: Inverse optimal adaptive control for attitude tracking of spacecraft. IEEE Transactions on Automatic Control 50(11), 1639–1654 (2005).
doi:10.1109/TAC.2005.858694.
2. Gennaro, S.D.: Output stabilization of flexible spacecraft with active vibration suppression. IEEE Transactions on Aerospace and Electronic Systems 39(3), 747–759 (2003).
doi:10.1109/TAES.2003.1238733.

3. Wang, H., Liu, P.X., Zhao, X. and Liu, X.: Adaptive fuzzy finite-time control of nonlinear systems with actuator faults. IEEE transactions on cybernetics 50(5), 1786-1797 (2020). doi:10.1109/TCYB.2019.2902868.
4. Kristiansen, R., Nicklasson, P.J., Gravdahl, J.T.: Spacecraft coordination control in 6DOF: Integrator backstepping vs passivity-based control. Automatica 44(11), 2896–2901 (2008). doi:10.1016/j.automatica.2008.04.019.
5. Shen, Q., Wang, D., Zhu, S., Poh, E.K.: Integral-type sliding mode fault-tolerant control for attitude stabilization of spacecraft. IEEE Transactions on Control Systems Technology 23(3), 1131–1138 (2015). doi:10.1109/TCST.2014.2354260.
6. Dong, L., Yan, J., Yuan, X., He, H. and Sun, C.: Functional nonlinear model predictive control based on adaptive dynamic programming. IEEE Transactions on Control Systems Technology 49(12), 4206-4218 (2019). doi:10.1109/TCYB.2018.2859801.
7. Angelis, E.L.D., Giulietti, F., Avanzini, G.: Single-axis pointing of underactuated spacecraft in the presence of path constraints. Journal of Guidance, Control, and Dynamics 38(1), 143–147 (2015). doi:10.2514/1.G000121.
8. Mclnnes, C.R.: Large angle slew maneuvers with autonomous sun vector avoidance. Journal of Guidance, Control, and Dynamics 17(4), 875–877 (1994). doi:10.2514/3.21283.
9. Lee, U., Mesbahi, M.: Feedback control for spacecraft reorientation under attitude constraints via convex potentials. IEEE Transactions on Aerospace and Electronic Systems 50(4), 2578–2592 (2014). doi:10.1109/TAES.2014.120240.
10. Shen, Q., Yue, C., Goh, C.H.: Velocity-free attitude reorientation of a flexible spacecraft with attitude constraints. Journal of Guidance, Control, and Dynamics 40(5), 1293–1299 (2017). doi:10.2514/1.G002129.
11. Kang, Z., Shen, Q., Wu, S.: Constrained attitude control of over-actuated spacecraft subject to instrument pointing direction deviation. IEEE Control Systems Letters 5(6), 1958–1963 (2021). doi:10.1109/LCSYS.2020.3044984.
12. Wie, B., Lu, J.: Feedback control logic for spacecraft eigenaxis rotations under slew rate and control constraints. Journal of Guidance, Control, and Dynamics 18(6), 1372–1379 (1995). doi:10.2514/3.21555.
13. Hu, Q., Li, B. and Zhang, Y.: Robust attitude control design for spacecraft under assigned velocity and control constraints. ISA transactions 52(4), 480–493 (2013). doi:10.1016/j.isatra.2013.03.003.
14. Li, M., Hou, M. and Yin, C.: Adaptive attitude stabilization control design for spacecraft under physical limitations. Journal of guidance, control, and dynamics 39(9), 2179-2183 (2016). doi:10.2514/1.G000348.
15. Shen, Q., Yue, C., Goh, C.H., Wu, B. and Wang, D.: Rigid-body attitude tracking control under actuator faults and angular velocity constraints. IEEE/ASME Transactions on Mechatronics 23(3), 1338-1349 (2018). doi:10.1109/TMECH.2018.2812871.

16. Shen, Q., Yue, C., Goh, C.H., Wu, B., Wang, D.: Rigid-body attitude stabilization with attitude and angular rate constraints. Automatica 90, 157–163 (2018). doi:10.1016/j.automatica.2017.12.029.
17. Shen, Q., Wang, D., Zhu, S., Poh, K.: Finite-time fault-tolerant attitude stabilization for spacecraft with actuator saturation. IEEE Transactions on Aerospace and Electronic Systems 51(3), 2390–2405 (2015). doi:10.1109/TAES.2015.130725.
18. Khalil, H.K.: Adaptive output feedback control of nonlinear systems represented by input-output models. IEEE Transactions on Automatic Control 41(2), 177–188 (1996). doi:10.1109/9.481517.
19. Khalil, H.: Nonlinear Systems (3rd Ed.). NJ: Prentice-Hall, Upper Saddle River (2002). doi:10.1016/s0005-1098(01)00289-8.
20. Wie, B.: Space Vehicle Dynamics and Control. American Institute of Aeronautics and Astronautics (2008). doi:10.2514/4.860119.